Construction and Building Materials 457 (2024) 139210

Contents lists available at ScienceDirect

Construction and Building Materials

journal homepage: www.elsevier.com/locate/conbuildmat

# Assessment of fiber alignment through combined driven oscillatory and directional magnetic fields in matrix with similar rheological behavior to cementitious materials

Nelson Flores Medina [a,*], Laura Trigo Ramirez [a], Víctor Pérez Villar [a], Víctor M. Cabrera García [a], Francisco Gil Carrillo [b]

[a] Departamento de Construcción Arquitectónica, Campus Universitario de Tafira, s/n, Las Palmas de Gran Canaria, Gran Canaria 35017, Spain
[b] Departamento de Construcciones Arquitectónicas y su control, Escuela Técnica Superior de Edificación, Universidad Politécnica de Madrid, Spain

ARTICLE INFO

*Keywords:*
Fiber alignment
Viscoelasticity
Directional magnetic field
Oscillatory magnetic field
Homogeneous magnetic field
Static Yield Stress

ABSTRACT

In this paper a novel method to improve the effectiveness of the aligning of fibers used as reinforcement in Fiber Reinforced Cementitious Composites (FRCC) through directional homogeneous magnetic fields is proposed. A combination of homogeneous magnetic fields, oscillatory and directional, are assessed as a new method for fiber aligning which increase the aligning index and mechanical efficiency index of the fiber in cementitious composites. Fresh cementitious materials present a Static Yield Stress ($T_0^s$), which must be overpassed to allow the rotation of the fiber immersed in the matrix. To reduce the $T_0^s$ of the matrix, oscillatory magnetic fields (OMF) are applied firstly, as they generate a vibrational strain of the fiber. Later, fibers are aligned through a directional magnetic field which finds a lower opposition of the rheological torque. The fibers are subjected to an orientation rotation caused by the magnetic field, which is caused by a magnetic torque. This torque is opposed by two torques, one of rheological origin (Yield stress and viscosity) and another of inertial type (geometry and mass distribution of the fiber). The rheological torque is the torque that opposes to the rotation of the fiber and is a function of the rheological properties of the matrix. Two pairs of Helmholt coils have been used in this research, to be able to generate orthogonal magnetic fields to directional magnetic fields. When the OMF was generated, one of the pair of coils were connected to the net, with a frequency of 50 Hz. OMF was performed in 0.64mT-1.25mT-2.18mT. To evaluate its effectiveness each of them was applied in periods of time of 2–5–7–10 seconds before the directional magnetic field of 30 mT. To assess the method steel fibers has been submerged in a metaphor fluid to reproduce the rheological properties of cement materials. The initial and final angles of the batch of fibers have been determined through photography and Computer-aided design. The results obtained shown that the use of OMF increases the alignment index up to 35 % and the mechanical efficiency rate up to 24.35 % in the batches studied. The research followed also showed that previous vibration can be applied during periods of 5 seconds, with the same pair of coils that for aligning but also the use of the two pair of coils can be used simultaneously.

## 1. Introduction

Cementitious materials are known as very durable and resistant materials but with a brittle failure under mechanical stress [1]. Steel fibers has been used as a reinforcement in cementitious materials to enhance the mechanical properties, but more in special their ductility and tenacity, increasing the number of cracks (but lower width) as the stress is therefore spread along the sample [2]. To optimize the work of fibers, they can be orientated through several methods, coming from an isotropic composite to an anisotropic composite. This aligning of fibers increases the mechanical properties when the direction of the stress is the same as the direction of the fiber, but also electrical, piezoelectric, thermal, etc. [3,4].

On the other hand, the addition of fibers also modifies the rheological behavior of the composite, increasing its Static Yield Stress ($T_0^s$), and its viscosity, arranging a maximum volume fraction (VF) to be able of

* Correspondence to: Campus Universitario de Tafira, s/n, Las Palmas de Gran Canaria, Gran Canaria 35017, Spain.
*E-mail address:* nelson.flores@ulpgc.es (N.F. Medina).

https://doi.org/10.1016/j.conbuildmat.2024.139210
Received 18 July 2024; Received in revised form 22 October 2024; Accepted 12 November 2024

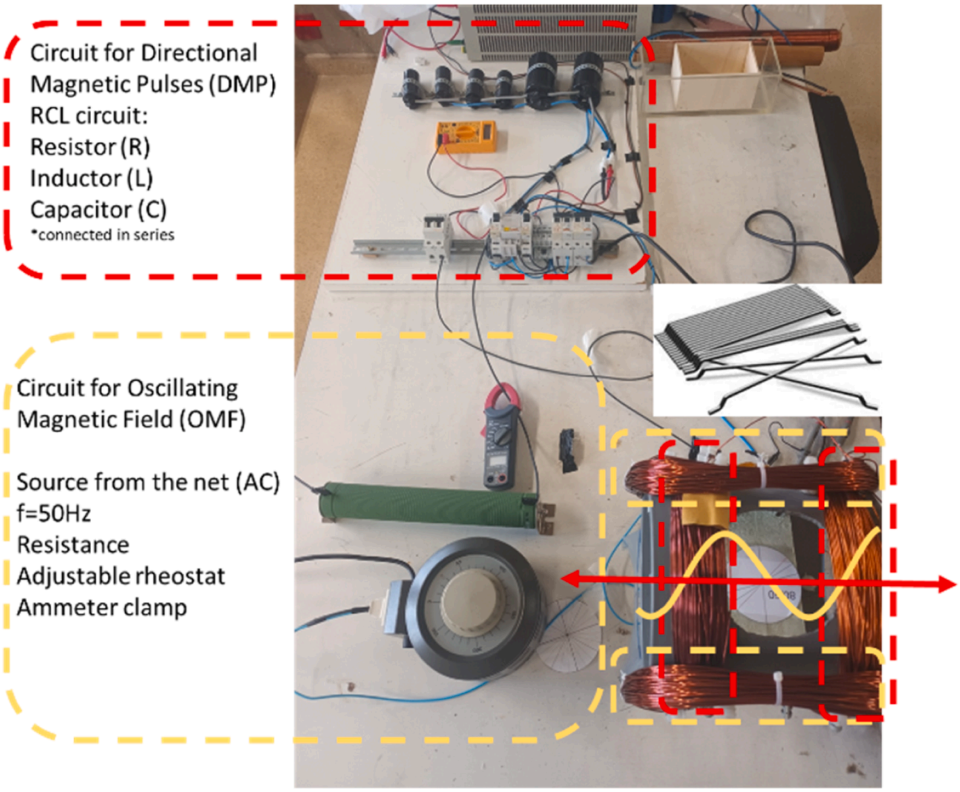


**Fig. 1.** Image of the 2 circuits used to align fiber and the two pairs of orthogonal Helmholtz coils.

**Table 1**
Magnetic field generated by the DMP system.

| $V_0$ (V) | $I_{max}$ (A) | $\mu_0H$ (RMS) | $B_{max}$ (mT) | $B_{RMS}$ (mT) |
|---|---|---|---|---|
| 100 | 21 | 30 | 43.33 | 20.61 |

workability. This VF of fibers usually is around 1.5 % depending on the size of the fiber, its flexibility, properties of the matrix but also to the risk of entanglement between fibers, also known as balling-up. However, when fibers are in a composite after casting the fibers must overpass the $T_0^s$ of the matrix, as in a matrix with the VF of fibers in a random and homogeneous distribution in the composite are distanced from others [5].

Cementitious matrices present a $T_0^s$, which may reach low values with the appropriate use of superplasticizers and fine additions [2]. $T_0^s$ is caused by the internal forces in the matrix (colloidal and frictional) that keeps in repose of the fluid the consistency and appearance of an elastic material. During vibration, if strong enough to overpass $T_0^s$, the matrix behaves as a fluid. When the vibration is stopped, the fluid recovers as a solid again. That point is considered the Dynamic Yield Stress ($T_0^d$) and the reduction of stress to achieve again the viscous behavior is considered thixotropy. After some time depending on the matrix, the initial conditions are again set up However, they behave as Bingham or Herschel-Bulkley proper of a viscoelastic fluid, but also show a thixotropic behavior or recently more precise a built-up structure [6–8]. Hence, the rheological behavior of cementitious composites becomes complex, which rheological properties have been deeply studied considering the time under rest but also after a stimulus (incitement) such as compaction, flow, vibration.

Thixotropy is considered as the reversible effect observed as a continuous decrease of viscosity with time when flow is applied to a dispersion that has been previously at rest and the subsequent recovery of viscosity in time when the flow is discontinued [9]. Hysteresis loops can be used to determine the thixotropy of a dispersion, and it is considered as the area enclosed in it obtained by increasing and decreasing the shear rate from zero to a maximum, plotted in a shear stress versus shear rate diagram. Thixotropy can be caused by relatively weak attractive forces between particles forming flocs which can be broken during flow [8,9]. When flow is reduced, flocs can grow again and increase the viscosity of the dispersion. When the flow is arrested the particulate network can be rebuilt, as a reversible.

Some dispersions, like cementitious pastes and mortars, present a thixotropic-like behavior which is known as structural-built up [7,8]. These fluids present reversible but also irreversible effects, increasing these lasts with time as the $T_0^s$ is also increased.

However, when the mass is cast the viscoelastic properties of the matrix can be more decisive to obtain fiber alignment as they show solid state behavior up to a certain stress. The dispersion material when viscoelastic stores elastic potential energy upon an application of strain over timescales comparable to observation timescale. The time when stress relaxes is termed as relaxation time of a mater [10]. To assess the viscoelastic domain of a matrix, low strain tests can determine the storage modulus (G′) in the elastic domain when the matrix can be considered a solid network and the loss modulus (G″) in the viscous domain when the matrix can be considered as a liquid. A real material has a viscoelastic behavior, G′and G″are finite. The material can exhibit a solid-like behavior, with G′>>G″, or a liquid-like one, with G″<<G′ [6].

The elastic domain of many matrices can be modified using vibration of the fibers at low strain, reducing the storage modulus as deflocculation and particle migration can occur [11]. The reduced storage modulus allows the fiber to move or rotate easier as the matrix reduces its elastic domain and the static yield stress that must be overpassed is lower. The elastic domain is characterized in static forces below the $T_0^s$ meanwhile, and in oscillatory forces caused for example through vibrational forces in low strain through G′. [6]

Hysteresis in viscoelastic materials is observed because of the finite time required by the same to reach the steady state corresponding to the applied flow field, which is governed by the magnitude of their

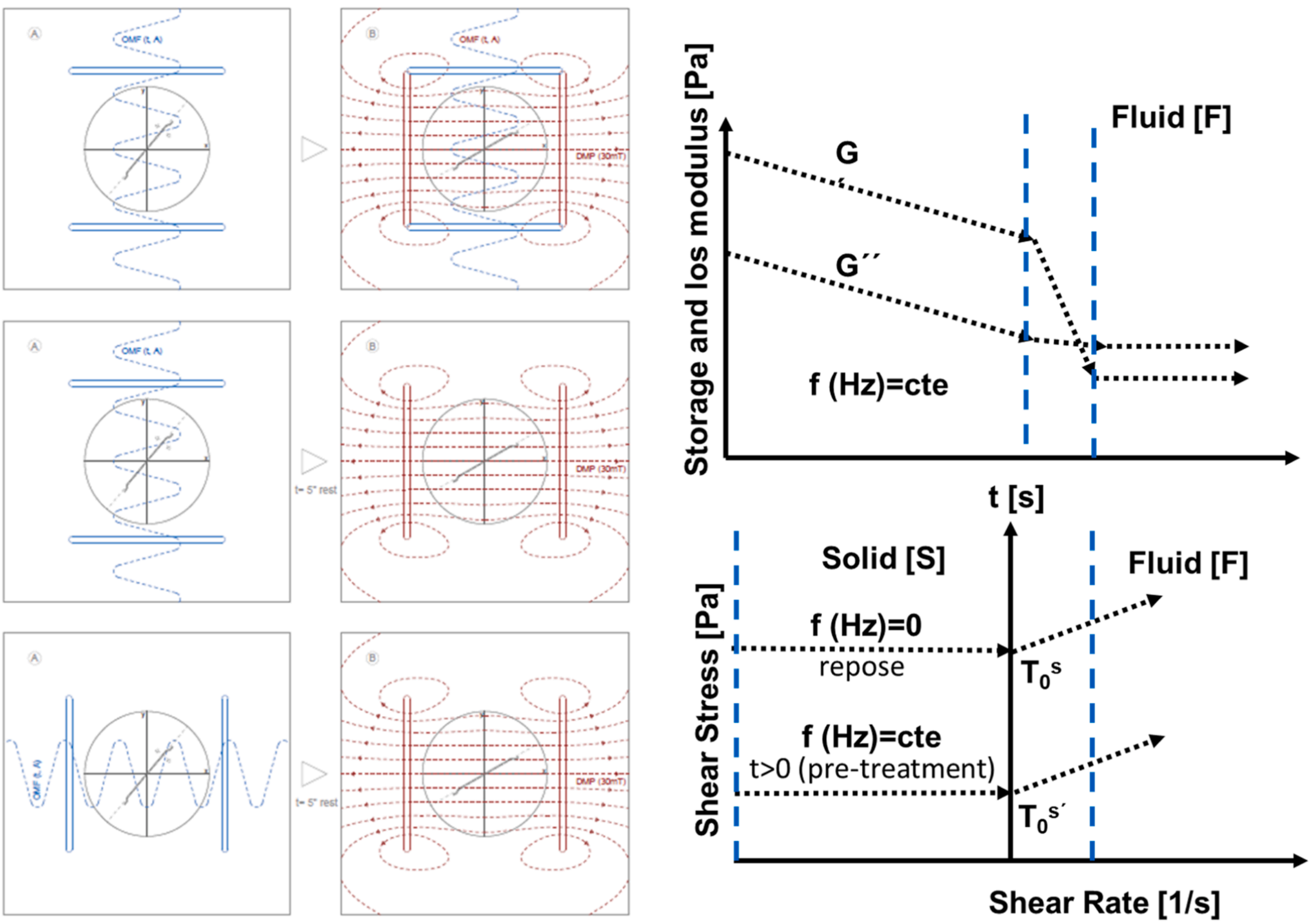


**Fig. 2.** Schematic representation of the different procedures to evaluate the effectiveness of the method combining OMF and DMP.

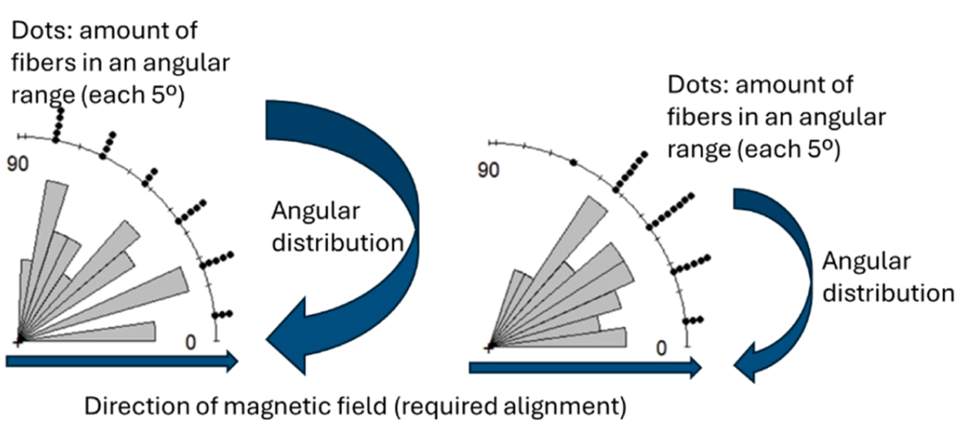


**Fig. 3.** Graphical representation of circular statistics (rose diagram).

relaxation time. Consequently, if the sweep rate is faster than the relaxation time of the material, then due to incomplete relaxation of stress during down-sweep and incomplete buildup of stress during up-sweep, shear stress does not trace the same path in the do/n-sweep and up-sweep shear flow [10]

The magnetic alignment of fibers as reinforcement in cementitious composites has been studied previously using a directional magnetic field alone or combined with mechanical vibration (vibrational table) [12–23]. The magnetic devices may be formed by a simple coil, a pair of coils following a Helmholtz distribution, but also some studies use ferromagnetic blocks. When Helmholtz coils are used a homogeneous magnetic field is presented and only rotational torques are generated to the ferromagnetic fibers in the composite. In a previous research work [24], fiber alignment in a Bigham matrix through short time homogeneous magnetic pulses ($t \approx 0.2$ s) with different intensities in one direction, directional magnetic pulses (DMP), was studied alone. It was observed the importance of the initial angle θ between the fiber and the magnetic field H, the shape factor and flexibility of fiber, as they interact with the rheological properties of the matrix. Hence, to rotate the fibers with an angular velocity θ, the magnetic torque must overpass the rheological torque $\Upsilon_R$, especially affected by the initial value of static tress $T_0^{(d)}$ and dynamical one To$^{d}$) as stated in a previous works [24,38]

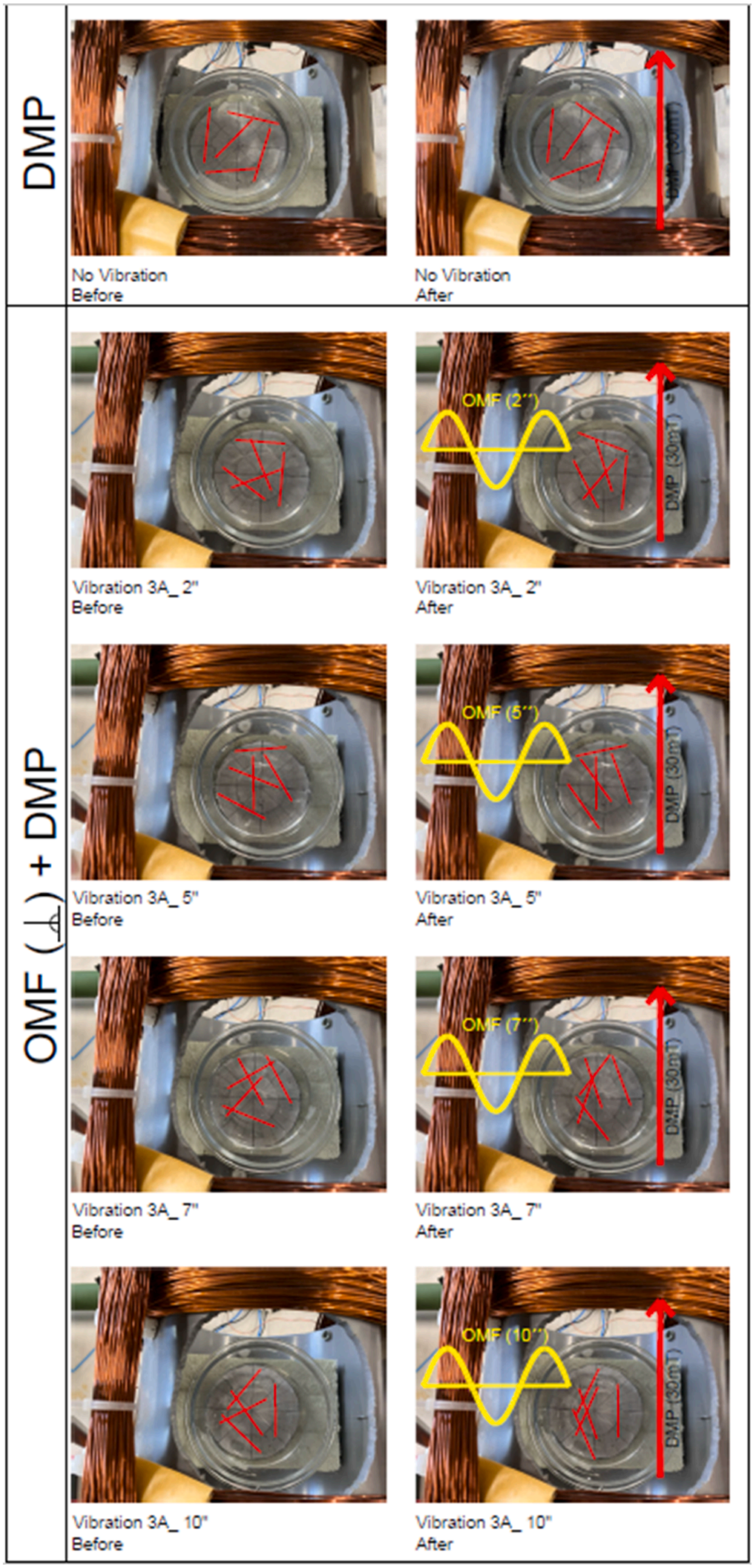


**Fig. 4.** Images of the fibers in Carbopol with CAD analysis in samples aligned with DMP alone and samples with DMP+OMF.

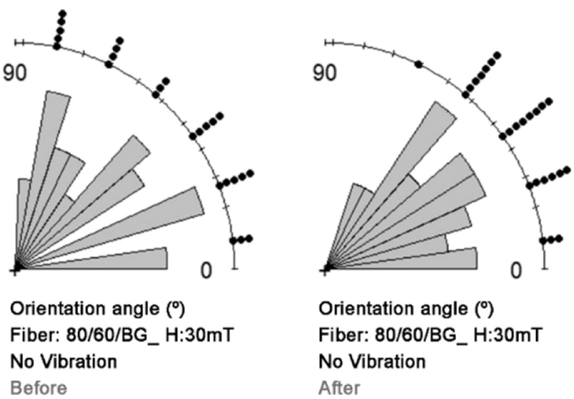


**Fig. 5.** Angular distribution through circular statistics of fiber 80/60/BG before/after DMP under RMS magnetic inductance of 30mT from coil.

(Eq. 1).

$$\underbrace{\ell S|\overrightarrow{H}(t)|H_B(|\overrightarrow{H}(t)|\cos\theta)\sin\theta}_{Magnetic\ Torque} = \underbrace{\Upsilon_R(S_{f0,}T_0^{(d)},T_0^{(e)},\dot{\theta})}_{Rheo\ \log\ ical\ Torque} + \underbrace{I\ddot{\theta}}_{Inertia} \quad (1)$$

where the intensity of the magnetic field H coming from the coil, the angle θ, the section S and the length of the fiber l are considered, and the moment of inertia I as well. In the same way, the ferromagnetic response H as function called hysteresis cycle of fiber is included in the dynamical response equation of fiber.

Attending to the properties of the matrix, in this work a combined method to align fibers through two different homogeneous magnetic fields, oscillating and DMP, is studied. The oscillating magnetic field is proposed to modify the properties of the fluid in the elastic domain by the vibration of the fiber in the matrix. The vibration of fibers during several seconds before the second magnetic field is activated reduces the $T_0^s$. Later, when $T_0^s$ is modified, as fibers may find lower opposition to rotate DMP is applied. This novel method has been studied using different times of exposure and magnetic field values, but also in two pair of coils or one pair of coils. To set properly the ranges of alignment depending on fiber angle, a transparent viscoelastic fluid was used as a metaphor of a cementitious material, which has been also studied with grains [25].

There are specific studies on the mechanical improvement in cementitious materials with steel fiber on samples irradiated with magnetic inductions of approximately 0.5 T, a recent study [12] shows an improvement increased the compressive strength of cube and cylinder specimens up to 18.23 and 12.03 %, respectively. Magnetic orientation in fibers increased flexural strength by up to 50 % according with [21]. Magnetic orientation of steel fibers in transparent silicone oil and in fresh, self-compacting concrete (SCC) beams is studied experimentally in [16] showing a greater bending tensile strength and energy absorption capacity.

This work is motivated by the need for a method to increase the effectiveness of the magnetic alignment methods to achieve the rotation of fibers not only by the increase of the magnetic field but also by understanding and reducing the Yield Stress of the of the cementitious materials. The future objective of this study is to analyze the method in cementitious matrices with $T_0^s$ modified using vibration treatment through magnetic fields.

## 2. Test method

The method followed continues with the procedures and materials from a previous research work, which DMP in one axis was applied.[24] The materials used are:

### 2.1. Metaphor matrix

A transparent matrix, Carbopol® 940, was selected as a metaphor fluid to cementitious materials [24–26]. Carbopol allows to set a batch of tests, measuring the angle of several fibers before and after the magnetic alignment is applied, allowing the comparison of angular rotation for each initial disposition of the fiber. It has been used previously by the authors and other researchers as metaphor fluid for cementitious materials [24–29]. Carbopol® samples exhibit visco-elastoplastic properties: shear thinning behavior under an applied strain rate (or shear stress) and a yield stress, over which flow and plastic deformations occur [27]. Carbopol concentration and pH was settled to obtain a $T_0$ of 10 Pa [28,40]. This $T_0^s$ can be similar to several matrices used in composite material for mechanical purposes, such as cement paste, mortar or self compacting concrete [29]. Carbopol has the advantage of being able to be tuned in some rheological properties of static stress yield, by aqueous concentration of hydrogel [40].

The hydrogel matrix was prepared at 25 °C in two stages. Firstly, hydrating the sample by agitation with a magnetic stirrer at 600 rpm. Once the sample is completely dissolved, the dispersion is left static for 30 minutes for full hydration and elimination of any air bubbles that may have been generated during stirring. Secondly, the PH neutralization is done by adding triethanolamine (C6H15NO3) during gentle agitation to avoid air bubbles formation. The dispersion stays resting during 24 h before testing.

### 2.2. Fibers

A hooked-end fiber 80/60/BG, from the DRAMIX 3D series manufactured by Bekaert™ was used during the tests. The fiber was made of steel with a Young Modulus of 210000 MPa and presents a shape factor (l/d) of 80, with 60 mm length and 0.75 mm diameter and a mass of 0.22 g.

### 2.3. Magnetic aligning device and test procedure

Two orthogonal Helmholtz were manufactured along the perimeter of a PVC plastic cylinder and diameter 160 mm as structure with a coil of 16 AWG copper coated wire and width diameter of 1.5 mm, and a

**Table 2**
Statistical analysis of fiber alignment through circular statistical study of batches under DMP aligning method.

| DMP | | | | | | | | | | | | | | |
|---|---|---|---|---|---|---|---|---|---|---|---|---|---|---|
| Fibre | Sequence+ Exp Time (s) | Intensity (A) | μ0H (RMS) | N | sinϑ | cosϑ | $\bar{\theta}$ | $\bar{R}$ | Standard Desviation | Initial Angle 1st Quartile | Initial Angle 2nd Quartile | Initial Angle 3rd Quartile (Median) | Initial Angle 4th Quartile | Final Angle 4th Quartile |
| 80/ 60/ BG | Before | - | 30 mT | 25 | 0.6224 | 0.6581 | 43.4048 | 0.9058 | 0.4448 | 1 | 19,00 | 41,00 | 67,00 | 85,00 |
| 80/ 60/ BG | After | - | 30 mT | 25 | 0.5266 | 0.7927 | 33.5951 | 0.9516 | 0.3149 | 1 | 17,00 | 34,00 | 49,00 | 70,00 |

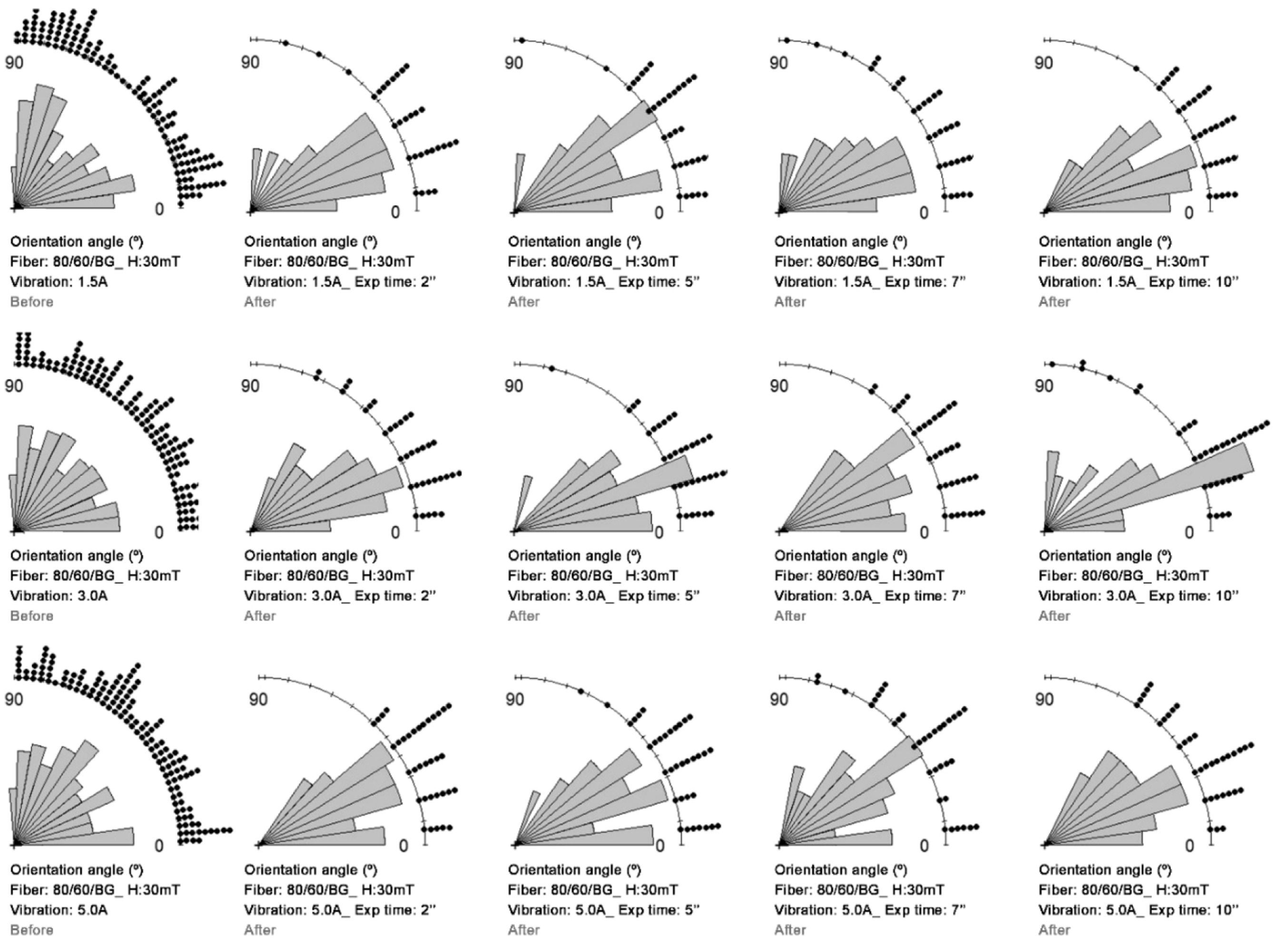


**Fig. 6.** Angular distribution through circular statistics of fiber 80/60/BG before and after orthogonal oscillatory magnetic fields and applied simultaneously with DMP of 30mT magnetic induction from coil.

winding of 100 loops (Fig. 1). One pair of coils was used to obtain a (DMP), setting a magnetic field of 30mT in every test. The value of magnetic field inside of the coil was determine using the Maxwell Equations (Ampere's law) were used and published in a previous work [9]. The peak electric intensity ($I_{Max}$) generated during the discharge and also the peak of the magnetic field ($B_{Max}$), together with the RMS (Root Mean Square) value $B_{RMS}$ of such magnetic field peak generated by the Hemholtz Coil are summarized in Table 1:

The other pair of coils was used to obtain an oscillating magnetic field (OMF). The oscillating field was obtained by the use of the electrical supply from the net at 50 Hz and 220 V, setting the adequate amperage through the use of an adjustable rheostat and a ammeter clamp (Fig. 1). The magnetic field was set at three different amperages,1.5–3–5 A which showed a value of 0.64mT-1.25mT-2.18mT respectively. The magnetic field was measured with a Gaussmeter, model GM07/08 from the Hirst Magnetic Instruments Ltd. with a hall probe. The testing procedures were named as follows: Vibration 3A_10"": Vibration at 3 Amperes after 10 seconds.

Both systems were used following the following procedures (Fig. 2):

1. OMF was firstly activated at a desired amperage and for a determined period in a perpendicular pair of Helmholtz coils and simultaneously DMP was activated.
2. OMF was firstly activated at a desired amperage and for a determined period in a perpendicular pair of Helmholtz coils and after 5 seconds DMP was activated.
3. OMF was firstly activated at a desired amperage and for a determined period in a the same direction and after 5 seconds DMP was activated.

### 2.4. Circular statistics

To study the angular distribution of fibers obtained through Computer Aided Design (CAD) analysis of the images, circular statistics has been used [30,31]. The angle between the fiber and the magnetic field direction was measured before and after the magnetic field was applied. For this, the fibers were drawn in CAD as shown in Fig. 3 and the angles settled from the pictures of the process. From this study several advantages can be obtained. Firstly, the graphical representation of the results obtained and its interpretation. Secondly, the homogeneity of the composite in terms of angular distribution can be easily determined, through its distribution in quartiles, the median, and the spread of the samples through the centroid.

$$(\sin\theta_i,\ \cos\theta_i) \quad i = 1, \dots, n \tag{2}$$

The Cartesian coordinates of the "center of mass" ($\widehat{R}$ can be obtained:

$$\widehat{S} = \frac{1}{n}\sum_{i=0}^{n}\sin\theta i \tag{3}$$

$$\widehat{C} = \frac{1}{n}\sum_{i=0}^{n}\cos\theta i \tag{4}$$

**Table 3**
Statistical analysis of fiber alignment through circular statistical study of batches under orthogonal oscillatory magnetic fields and simultaneous DMP.

| Ortoghonal alternating magnetic field+simultaneous DMP | | | | | | | | | | | | |
|---|---|---|---|---|---|---|---|---|---|---|---|---|
| Fibre | Sequence+ Exp Time (s) | Intensity (A) | μ0 H (RMS) | N | sinϑ | cosϑ | $\overline{\theta}$ | $\overline{R}$ | Standard Desviation | Initial Angle 1st Quartile | Initial Angle 2nd Quartile | Initial Angle 3rd Quartile (Median) |
| 80/60/BG | Before | 1.5 | 30 mT | 135 | 0.64 | 0.6095 | 46.3967 | 0.8838 | 0.4970 | 0.00 | 18.00 | 44.00 |
| 80/60/BG | After_ 2" | 1.5 | 30 mT | 30 | 0.4761 | 0.8298 | 29.8421 | 0.9567 | 0.2976 | 3.00 | 20.25 | 29.50 |
| 80/60/BG | After_ 5" | 1.5 | 30 mT | 35 | 0.4740 | 0.8335 | 29.6271 | 0.9589 | 0.2899 | 3.00 | 15.50 | 32.00 |
| 80/60/BG | After_ 7" | 1.5 | 30 mT | 35 | 0.4708 | 0.8126 | 30.0882 | 0.9392 | 0.3542 | 0.00 | 15.00 | 28.00 |
| 80/60/BG | After_ 10" | 1.5 | 30 mT | 35 | 0.4121 | 0.8744 | 25.2320 | 0.9667 | 0.2604 | 3.00 | 12.50 | 24.00 |
| 80/60/BG | Before | 3.0 | 30 mT | 140 | 0.6305 | 0.6297 | 45.0381 | 0.8911 | 0.4803 | 0.00 | 22.75 | 43.00 |
| 80/60/BG | After_ 2" | 3.0 | 30 mT | 35 | 0.4691 | 0.8343 | 29.3264 | 0.9571 | 0.2962 | 5.00 | 18.00 | 26.00 |
| 80/60/BG | After_ 5" | 3.0 | 30 mT | 35 | 0.3796 | 0.8853 | 23.2092 | 0.9633 | 0.2734 | 1.00 | 11.00 | 21.00 |
| 80/60/BG | After_ 7" | 3.0 | 30 mT | 35 | 0.4202 | 0.8693 | 25.8008 | 0.9655 | 0.2648 | 0.00 | 14.50 | 28.00 |
| 80/60/BG | After_ 10" | 3.0 | 30 mT | 35 | 0.4599 | 0.8192 | 29.3074 | 0.9395 | 0.3534 | 0.00 | 20.00 | 28.00 |
| 80/60/BG | Before | 5.0 | 30 mT | 140 | 0.6418 | 0.6246 | 45.7820 | 0.8956 | 0.4697 | 0.00 | 24.50 | 50.00 |
| 80/60/BG | After_ 2" | 5.0 | 30 mT | 35 | 0.432 | 0.8714 | 26.3684 | 0.9726 | 0.2356 | 1.00 | 18.00 | 29.00 |
| 80/60/BG | After_ 5" | 5.0 | 30 mT | 35 | 0.4418 | 0.85534 | 27.3718 | 0.9610 | 0.2822 | 1.00 | 18.50 | 28.00 |
| 80/60/BG | After_ 7" | 5.0 | 30 mT | 35 | 0.5334 | 0.7775 | 34.4515 | 0.9428 | 0.3432 | 0.00 | 23.50 | 35.00 |
| 80/60/BG | After_ 10" | 5.0 | 30 mT | 35 | 0.4847 | 0.8396 | 20.2640 | 0.9617 | 0.2795 | 2.00 | 17.50 | 27.00 |

The component $\widehat{C}$ obtained from Eq. 4 is considered the alignment index. Hence, in directional the alignment index is already included. The vector of the center of mass provides the fiber orientation and the length provides the spread of the batch studied, the values near 0 indicate a high spread of the sample and the closer to 1 the nearest to the main angle and hence the angular homogeneity of the reinforcement of the composite:

$$\widehat{R} = \overrightarrow{R} = \sqrt{\widehat{S}^2 + \widehat{C}^2} \quad (5)$$

$\overrightarrow{R}$ Where R value (centroid) is considered as dispersion value of the circular data if R is zero the data is homogeneous dispersed and 1 is considered as concentrated near to the angular mean value, the circular mean orientation of fibers, which is obtained from the following expression:

$$\overline{\theta} = \arctan\frac{\widehat{S}}{\widehat{C}} \quad (6)$$

In this way, the lower the amplitude of quartiles 2 and 3, the more concentrated is the batch of fibers studied. The median represents the main angular direction of the batch of fibers attending to its distribution in each bit of 5º from 0º to 90º, being 90º for an isotropic but normal to the desired direction, 45º usually for anisotropic and 0º for a an isotropic in the desired direction (the direction of the DMP). The centroid allows us to set the spread of the sample, being a 0 value totally anisotropic and 1 totally isotropic. Fig. 2a shows a graphical representation of the results obtained through circular statistics. {{{Fig. 4}}}

### 2.5. Alignment index and mechanical efficiency factor (aka Cox-Krenchel Efficiency)

Fiber alignment in concrete and other Fiber Reinforced Cementitious Composites (FRCC) is estimated usually in the general literature of the topic through equation 04. This equation indicates the fiber alignment $\eta^{\theta}$, to angle 0º as the desired angle of orientation. When $\eta^{\theta}$is 0, fibers are badly aligned and present an orientation in the perpendicular direction to the one desired (isotropic 90º) and when is 1, fibers are well aligned (isotropic).

$$\eta^{\theta} = \frac{\sum_0^i \cos\sigma}{n} \quad (7)$$

To relate the fiber alignment and the composite mechanical characteristics, the mechanical efficiency factor ($\eta\theta_0$) following the Krenchel and Cox model has been applied [32,33]. To integrate this theory with directional statistics, if we divide the circumference into k bins, the following expression can be proposed:

$$\eta_{\theta_0} = \sum_k \chi_k \cos^4(\theta_k - \theta_0) \quad \text{Where} \quad \eta_\theta \in [0,1] \quad (8)$$

The reinforcement orientation distribution factor ranges between 0 (fibers aligned transverse to the stress direction) and 1 (fibers aligned parallel to the stress direction), the value of 3/8 (0.375) corresponds to randomly oriented fiber. FRC can be said to have ($\eta\theta_0$)=1 (100 %) the maximum reinforcement level for cracks perpendicular to the direction of the fibers.

The Krenchel and Cox model has been used as a prediction of the mechanical properties of fiber reinforced materials [39].

## 3. Results

The following figures present the fiber distribution in circular statistics. The distribution is set in the chart presenting graphically the number of fibers in bits of 5 grades from the angle 0º to 90º. The figures are ordered following the alternatives to the original method and its advanced proposals using oscillatory fields. First, the direct method with only a directional magnetic field of 30mT.

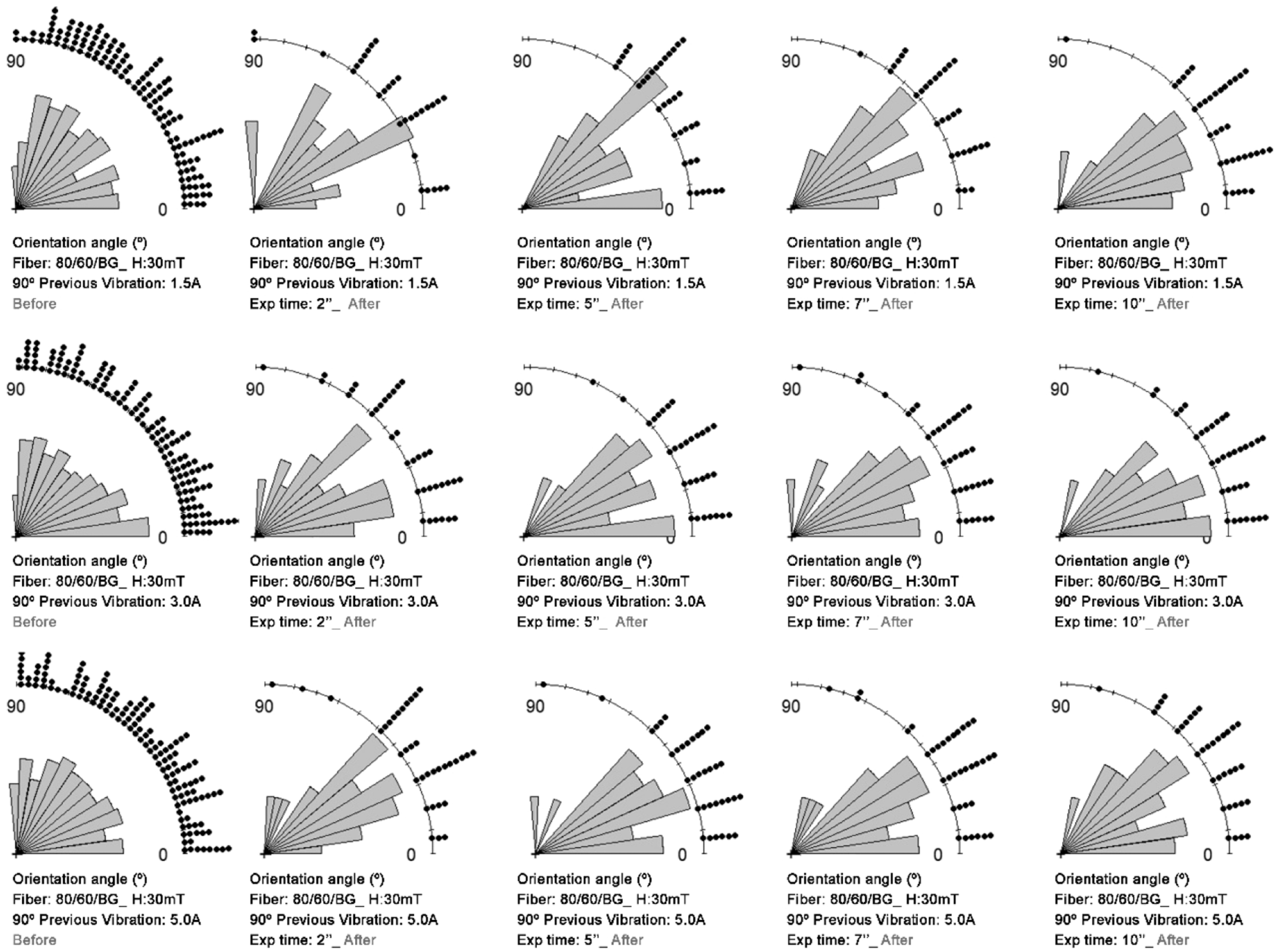


**Fig. 7.** Angular distribution through circular statistics of fiber 80/60/BG before and after a pretreatment with an orthogonal oscillatory magnetic field and DMP of 30mT induction from coil.

The results obtained in circular statistics of DMP with fiber 80/60/BG in the matrix studied are plotted in Fig. 5 and the main values are detailed in Table 2. The control batch with only DMP and the rest of the samples with OMF+DMP in different methods, time of exposure and amperage were studied with the statistical number of samples (fiber angles before and after. We can observe that the distribution of fibers before the DMP is applied is homogeneous, with an amplitude of 48º between second and third quartiles (it is the initial angle of the second quartile and the initial of the fourth quartile), and a median of 41º. The median is the final angle of the second quartile, same as the initial of the third quartile, as the authors indicate in the study only the final of the fourth and the initial of each quartile. DMP reduced the median to 34º and the amplitude of quartiles 2–3–32º.

In Fig. 6 the distribution of the fibers is presented when the oscillating field and the DMP are applied simultaneously. In this figure the oscillating field is obtained in a pair of coils perpendicular to those for the DMP. The results of this method are summarized in Table 3. The results present a reduction in the median and of the amplitude of the quartiles 2 and 3 when the oscillatory magnetic field is combined with DMP. In the case of oscillatory magnetic field of 1.5 A the median passes from 44º up to 24º, for 3.0 A from 43º to 21º, and for 5.0 A from 50 up to 27º. Concerning the amplitude of quartiles 2 and 3 the amplitude is reduced up to 18.5º when the oscillatory magnetic field is applied at 1.5 A, 16.5º when the OMF intensity is 3.0 A and 18º for 5.0 A. The lowest median, with a value of 21º was obtained through the use of the oscillatory field during 5 seconds, and for an intensity of 3 A. The lowest 2–3 quartiles amplitude was 16.5º for a OMF of 3.0 A during 10 seconds previously to DMP.

The use of two orthogonal magnetic fields, one for OMF and the other for DMP, using the OMF as a pretreatment of the matrix to reduce $T_0^S$ are plotted in Fig. 7 and the values obtained in Table 4. The results obtained show a reduction of the median from 48º up to 32º when the pretreatment is of 1.5 A in times of 5 and 10 seconds. The median is lowest for the 5 sec. pre-treatment with OMF at 3.0 A getting a median of 24º. With a OMF of 5.0 A as pretreatment of 5 sec., the median is reduced up to 28º. The amplitude of the quartiles is also lowest than before with the pretreatment with OMF, up to 26º for 7 sec. at 1.5 A, 22º for 3 sec. at 3.0 A and 20.5º for 7 sec. at 5.0 A.

In Fig. 8 the angular distribution of the fibers aligned through a pretreatment with oscillatory magnetic fields and later with the same coil a DMP is plotted. The results of the angular distribution are recorded in Table 5. It can be observed also a reduction of the median from 47º up to 28º when the OMF was used for 10 s. at an intensity of 1.5 A, up to 23º for 10 sec. at 3.0 A and up to 28º for 7 sec. at 5.0 A. The amplitude of the quartiles is also reduced by using this method, coming from 44.75º up to 21.5º for a pretreatment with a OMF of intensity 1.5 A., up to 22.5º for 3.0 A and up to 20.0º for 5.0 A.

## 4. Analysis and discussion

Comparing the results obtained with simple DMP and combined oscillatory and directional magnetic fields we can observe that the

**Table 4**
Statistical analysis of fiber alignment through circular statistical study of batches under a previous activation of an orthogonal oscillatory magnetic field and DMP.

| Orthogonal Pre-Alternating magnetic field + DMP | | | | | | | | | | | | |
|---|---|---|---|---|---|---|---|---|---|---|---|---|
| Fibre | Sequence+ Exp Time (s) | Intensity (A) | μ0 H (RMS) | N | sinϑ | cosϑ | $\bar{\theta}$ | $\bar{R}$ | Standard Desviation | Initial Angle 1st Quartile | Initial Angle 2nd Quartile | Initial Angle 3rd Quartile (Median) |
| 80/60/BG | Before | 1.5 | 30 mT | 130 | 0.6365 | 0.6429 | 44.7107 | 0.9047 | 0.4477 | 0.00 | 21.00 | 47.00 |
| 80/60/BG | After_ 2" | 1.5 | 30 mT | 30 | 0.5707 | 0.7323 | 37.9294 | 0.9285 | 0.3853 | 0.00 | 25.00 | 36.00 |
| 80/60/BG | After_ 5" | 1.5 | 30 mT | 35 | 0.5263 | 0.7982 | 33.3988 | 0.9560 | 0.2999 | 1.00 | 20.00 | 40.00 |
| 80/60/BG | After_ 7" | 1.5 | 30 mT | 30 | 0.5369 | 0.7968 | 33.9710 | 0.9608 | 0.2829 | 1.00 | 18.00 | 36.50 |
| 80/60/BG | After_ 10" | 1.5 | 30 mT | 35 | 0.4452 | 0.8475 | 27.7141 | 0.9573 | 0.2953 | 1.00 | 16.50 | 28.00 |
| 80/60/BG | Before | 3.0 | 30 mT | 135 | 0.5733 | 0.6776 | 40.2346 | 0.8876 | 0.4883 | 1.00 | 16.50 | 35.00 |
| 80/60/BG | After_ 2" | 3.0 | 30 mT | 35 | 0.4821 | 0.7987 | 31.1148 | 0.9329 | 0.3727 | 0.00 | 15.00 | 28.00 |
| 80/60/BG | After_ 5" | 3.0 | 30 mT | 30 | 0.4428 | 0.8497 | 27.5270 | 0.9582 | 0.2922 | 2.00 | 16.00 | 30.00 |
| 80/60/BG | After_ 7" | 3.0 | 30 mT | 35 | 0.4661 | 0.82 | 29.6165 | 0.9431 | 0.3420 | 2.00 | 17.00 | 29.00 |
| 80/60/BG | After_ 10" | 3.0 | 30 mT | 35 | 0.4191 | 0.8601 | 25.9810 | 0.9568 | 0.2972 | 1.00 | 13.00 | 23.00 |
| 80/60/BG | Before | 5.0 | 30 mT | 140 | 0.6197 | 0.6469 | 43.7715 | 0.8958 | 0.4691 | 0.00 | 21.00 | 44.50 |
| 80/60/BG | After_ 2" | 5.0 | 30 mT | 35 | 0.5285 | 0.7897 | 33.7899 | 0.9502 | 0.3195 | 0.00 | 22.00 | 29.00 |
| 80/60/BG | After_ 5" | 5.0 | 30 mT | 35 | 0.4407 | 0.8448 | 27.5507 | 0.9529 | 0.3108 | 1.00 | 17.00 | 29.00 |
| 80/60/BG | After_ 7" | 5.0 | 30 mT | 35 | 0.4533 | 0.8373 | 28.4268 | 0.9521 | 0.3132 | 0.00 | 17.00 | 28.00 |
| 80/60/BG | After_ 10" | 5.0 | 30 mT | 35 | 0.5139 | 0.8026 | 31.6298 | 0.9530 | 0.3103 | 1.00 | 19.00 | 33.00 |

median passes from 34º when DMP is applied as aligning method up to 20º for a combined method where the oscillating magnetic field is simultaneous and orthogonal to the DMP field. Same behavior is observed in the amplitude of 2 and 3 quartiles, where the amplitude recorded was reduced from 34º for DMP method up to 16.5º for Orthogonal Oscillatory field plus DMP.

This reduction of median and amplitude of quartiles results a higher aligning of the fibers to the desired direction and therefore a higher homogeneity of the angular distribution of the fibers. This is deeper analyzed in the following Tables 4–7, using the aligning index and the use of the mechanical efficiency rate explained in Section 2. The same order than for results has been developed during the analysis. First, the DMP methodology along has been analyzed and later the DMP combined with the OMF from different directions, times and moment in which is applied with DMP.

In Table 6 we can observe than DMP improves 16.97 % the alignment index, from the composite studied with random distribution of fibers and achieves an index value of 0.79. Concerning the mechanical efficiency rate, the increase obtained is of 17.52 % with a final value of 0.79.

In Table 7 the analysis obtained when the fibers are aligned through orthogonal OMF and simultaneous DMP in the same direction are presented. The highest alignment index achieved a 0.93 for OMF of 1.5 A after 10 seconds of application, with a 34.69 % improvement from the randomly destitution of fibers in the composite. In the same sample, the mechanical efficiency rate achieved a value of 0.87, what represents a increment of a 30.68 % of this rate compared to the initial distribution of fibers in the batch. However, when OMF was used with higher intensities (3.0 A and 5.0 A) the results are similar but lower. For instance, the maximum alignment index, with a value of 0.82, was obtained for the OMF at 3.0 A after 5 sec. with an mechanical efficiency rate 0.88. In the case of OMF at 5.A the alignment index achieved a value up to 0.87 after 3 sec. and an mechanical efficiency of 28.33.

Although the values are similar it can be observed that there might be an appropriate time for the use of the OMF as rheological treatment of the sample before the DMP is applied. This implies that for each matrix and type of fiber used, the coordination between time, intensity of the field and the viscoelastic or thixotropic properties of the matrix should be carefully studied. In the proceeding of the method here studied, the higher intensities of OMF seem to need to be used in shorter times for the matrix here studied, however for lower intensities the time must be or can be reduced.

On any case, it can be highlighted than the alignment indexes and mechanical efficiency rates are over that those obtained through the DMP method along, what indicates the improvement of the method proposed in this work. The mechanical efficiency rates are higher also thanks to the higher volume of fibers that rotated near the final alignment desired.

Continuing with the analysis and discussion of the method, but through another proceeding using a previous activation of an orthogonal OMF and later the DMP (Table 8). The results show an improvement of the aligning index up to 0.99 and Mechanical efficiency rate of 0.84 for an OMF at an intensity of 1.5 A after 10 seconds, up to 0.86 alignment index and 0.85 mechanical efficiency rate for an OMF at an intensity of 3.0 A during 10 sec. and up to 0.84 alignment index and a 0.84 mechanical efficiency rate for 5 seconds of OMF at 5.0 A. The maximum improvement obtained near a 35 % in the alignment index and a 24.35 % in the mechanical efficiency rate. In every case, the results show a better efficiency when the pretreatment with OMF plus DMP are used than only for DMP.

This is in accordance with hypothesis mentioned from the literature that after an effort, even under the $T_0^s$ value (Fig. 9right), this is later reduced as the microstructure of the matrix is affected by a relaxation of the material [34]. Several studies have shown that at determined frequencies, the material goes from a dominant elastic behavior to a dominant viscous behavior (Fig. 9left). This stress softening allows the

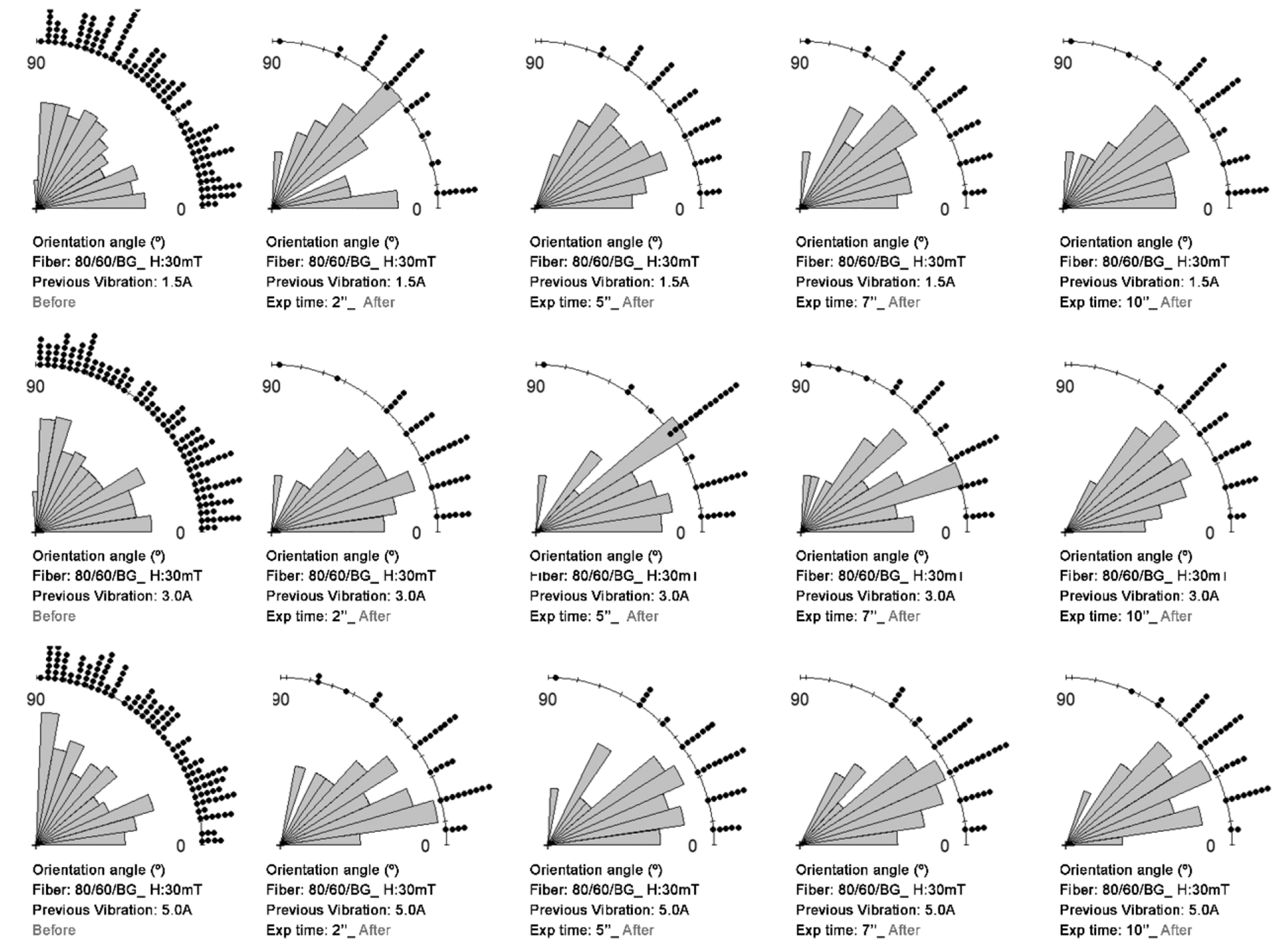


**Fig. 8.** Angular distribution through circular statistics of fiber 80/60/BG before and after a pretreatment with oscillatory magnetic induction and DMP of 30mT in the same direction.

rotation of the fiber with lower magnetic fields, or with the same magnetic field a higher angular response in the same fluid after pre-vibration treatment. However, the time of appliance of the stress to the matrix using the OMF is not linear, as some results obtained are better with lower times of pretreatment. The time of application of the DMP after the rheological pretreatment through OMF must be also taken in account in this process as the matrix may recover the microstructure and lose its beneficial effect [35]. In this proceeding the coordination of OMF time and the time for DMP should be studied for the matrix used in the composite.

In Table 9, the analysis of the results obtained by the same pair of coils, to apply first to the matrix a pretreatment with the OMF and later the DMP has been summarized. The higher alignment index and mechanical efficiency rate for 10 seconds of pretreatment with the OMF at 1.5 A got up to 0.80 and 0.79 respectively. In the case of the use of OMF at 3.0 A the alignment index got up to 0.85 and the mechanical efficiency rate up to 0.84, but OMF was used 2 sec. With the higher intensity for the OMF (5.0 A) the alignment index achieved a maximum of 0.85 and the mechanical efficiency rate of 0.84, after 7 seconds.

The results in this case were better when the OMF was used at 3.0 A and 5.0 A. This can be caused by the time between the OMF ending and the DMP application, in which the matrix recovers it rheological properties. In this sense, the higher intensity may have caused damages to the matrix for longer time and hence lower $T_0$ in the time when DMP was used [36]. The authors observed that in cases with high alignment indexes (over 80 %) the improvement obtained between the different amperages and times of exposure are not proportional to them. This may be caused by the rheological behaviour of the matrix and because the magnetic torque can reach a maximum value in high angular rotations as it is reduced when the angle between fiber and magnetic field is similar [24].

The analysis of the results with the mechanical efficiency rate indicates that the method of using a rheological OMF before DMP is better than DMP along. This means that the understanding of the rheological properties of the matrix must be studied in coordination with the DMP used. With a proper study of the rheological properties of the matrix and the intensity of the OMF and the time of exposure, this method can be applied in circumstances where the limitation of the DMP intensity do not manage a desired mechanical property of the composite. Moreover, it is necessary to set the T0s in the moment of application of the magnetic alignment, as cementitious materials show build-up behaviour during setting. The results obtained will be adequate for a determined time of manufacturing, what must be also determined with rheological testing.

The results obtained may indicate that the use of DMP should be as soon as possible to the moment of ending the application of OMF, as the processes studied with a pause of 5'' between OMF and DMP resulted in lower alignment coefficients. This can be caused by the recovery of the rheological properties of the matrix and hence partially the $T_0^s$. The process of using OMF and DMP simultaneously did not let time to the

**Table 5**
Statistical analysis of fiber alignment through circular statistical study of batches under a previous activation of oscillatory magnetic field and later a DMP in the same direction with same pair of coils.

| Pre-Alternating magnetic field + DMP | | | | | | | | | | | | |
|---|---|---|---|---|---|---|---|---|---|---|---|---|
| Fibre | Sequence+ Exp Time (s) | Intensity (A) | μ0 H (RMS) | N | sinϑ | cosϑ | $\bar{\theta}$ | $\bar{R}$ | Standard Desviation | Initial Angle 1st Quartile | Initial Angle 2nd Quartile | Initial Angle 3rd Quartile (Median) |
| 80/60/BG | Before | 1.5 | 30 mT | 140 | 0.6358 | 0.6288 | 45.3174 | 0.8942 | 0.4730 | 0.00 | 19.75 | 48.00 |
| 80/60/BG | After_ 2" | 1.5 | 30 mT | 35 | 0.563 | 0.7359 | 37.4180 | 0.9266 | 0.3905 | 0.00 | 19.50 | 42.00 |
| 80/60/BG | After_ 5" | 1.5 | 30 mT | 35 | 0.5307 | 0.7916 | 33.8406 | 0.9531 | 0.3101 | 4.00 | 20.00 | 32.00 |
| 80/60/BG | After_ 7" | 1.5 | 30 mT | 35 | 0.5213 | 0.7868 | 33.5243 | 0.9439 | 0.3399 | 0.00 | 17.00 | 35.00 |
| 80/60/BG | After_ 10" | 1.5 | 30 mT | 35 | 0.498 | 0.8036 | 31.7890 | 0.9454 | 0.3352 | 5.00 | 17.00 | 32.00 |
| 80/60/BG | Before | 3.0 | 30 mT | 140 | 0.6146 | 0.6391 | 43.8791 | 0.8867 | 0.4905 | 0.00 | 20.50 | 40.50 |
| 80/60/BG | After_ 2" | 3.0 | 30 mT | 35 | 0.425 | 0.851 | 26.5373 | 0.9512 | 0.3164 | 0.00 | 14.00 | 24.00 |
| 80/60/BG | After_ 5" | 3.0 | 30 mT | 35 | 0.4414 | 0.8454 | 27.5679 | 0.9537 | 0.3079 | 1.00 | 13.00 | 31.00 |
| 80/60/BG | After_ 7" | 3.0 | 30 mT | 35 | 0.5027 | 0.797 | 32.2441 | 0.9423 | 0.3448 | 4.00 | 19.50 | 25.00 |
| 80/60/BG | After_ 10" | 3.0 | 30 mT | 35 | 0.5044 | 0.8248 | 31.4435 | 0.9669 | 0.2597 | 0.00 | 20.50 | 33.00 |
| 80/60/BG | Before | 5 | 30 mT | 140 | 0.6574 | 0.6047 | 47.3934 | 0.8932 | 0.4753 | 1 | 21 | 47.5 |
| 80/60/BG | After_ 2" | 5.0 | 30 mT | 35 | 0.4911 | 0.8102 | 31.2243 | 0.9474 | 0.3286 | 1.00 | 15.50 | 30.00 |
| 80/60/BG | After_ 5" | 5.0 | 30 mT | 35 | 0.4673 | 0.8254 | 29.5138 | 0.9485 | 0.3252 | 1.00 | 16.00 | 28.00 |
| 80/60/BG | After_ 7" | 5.0 | 30 mT | 35 | 0.4619 | 0.8493 | 28.5394 | 0.9668 | 0.2600 | 1.00 | 17.00 | 28.00 |
| 80/60/BG | After_ 10" | 5.0 | 30 mT | 35 | 0.4968 | 0.8262 | 31.0177 | 0.9640 | 0.2708 | 0.00 | 18.00 | 32.00 |

**Table 6**
Alignment index and mechanical efficiency factor of fiber aligned through DMP aligning method.

| DMP | | | | | | |
|---|---|---|---|---|---|---|
| Fibre | Sequence+ Exp Time (s) | Intensity (A) | Alignment Index | Improvement Alingm.index (%) | Efficiency rate | Improvement Eff.Rate (%) |
| 80/60/BG | Before | - | 0.6581 | | 0.6486 | |
| 80/60/BG | After | - | 0.7927 | 16.97994197 | 0.7864 | 17.52 |

**Table 7**
Alignment index and mechanical efficiency factor of fiber aligned through orthogonal OMF and simultaneous DMP in the same direction.

| Orthogonal alternating magnetic field+simultaneous DMP | | | | | | |
|---|---|---|---|---|---|---|
| Fibre | Sequence+ Exp Time (s) | Intensity (A) | Alignment Index | Improvement Alingm.index (%) | Efficiency rate | Improvement Eff.Rate (%) |
| 80/60/BG | Before | 1.5 | 0.6095 | | 0.6038 | |
| 80/60/BG | After_ 2" | 1.5 | 0.8298 | 26.55 | 0.8239 | 26.71 |
| 80/60/BG | After_ 5" | 1.5 | 0.8335 | 26.87 | 0.8312 | 27.36 |
| 80/60/BG | After_ 7" | 1.5 | 0.8126 | 24.99 | 0.8068 | 25.16 |
| 80/60/BG | After_ 10" | 1.5 | 0.9332 | 34.69 | 0.8710 | 30.68 |
| 80/60/BG | Before | 3.0 | 0.6530 | | 0.6244 | |
| 80/60/BG | After_ 2" | 3.0 | 0.8343 | 21.73 | 0.8283 | 24.62 |
| 80/60/BG | After_ 5" | 3.0 | 0.8852 | 26.23 | 0.8792 | 28.98 |
| 80/60/BG | After_ 7" | 3.0 | 0.8693 | 24.88 | 0.8656 | 27.87 |
| 80/60/BG | After_ 10" | 3.0 | 0.8192 | 20.29 | 0.8156 | 23.44 |
| 80/60/BG | Before | 5.0 | 0.6246 | | 0.6208 | |
| 80/60/BG | After_ 2" | 5.0 | 0.8714 | 28.32 | 0.8662 | 28.33 |
| 80/60/BG | After_ 5" | 5.0 | 0.8534 | 26.81 | 0.8491 | 26.89 |
| 80/60/BG | After_ 7" | 5.0 | 0.7775 | 19.67 | 0.7718 | 19.56 |
| 80/60/BG | After_ 10" | 5.0 | 0.8306 | 24.80 | 0.8245 | 24.71 |

matrix to recover the initial properties through tixotrophy, as the DMP was applied when the matrix was still submitted to vibration. In this case the highest values of mechanical efficiency are obtained, as the percent of fiber that rotated is the highest and its mechanical collaboration in the composite will be then more active.

The higher mechanical efficiency here studied of the fiber reinforcement, will lead to a less cracking opening of the cementitious composite. The mechanical efficiency is linked to the coincidence of the

**Table 8**
Alignment index and mechanical efficiency factor of fiber aligned through a previous activation of an orthogonal oscillatory magnetic field and DMP.

| **Orthogonal Pre-Alternating magnetic field + DMP** | | | | | | |
|---|---|---|---|---|---|---|
| Fibre | Sequence+ Exp Time (s) | Intensity (A) | Alignment Index | Improvement Alingm.index (%) | Efficiency rate | Improvement Eff.Rate (%) |
| 80/60/BG | Before | 1.5 | 0.6429 | | 0.6374 | |
| 80/60/BG | After_ 2" | 1.5 | 0.7323 | 12.21 | 0.7297 | 12.65 |
| 80/60/BG | After_ 5" | 1.5 | 0.7982 | 19.46 | 0.7888 | 19.19 |
| 80/60/BG | After_ 7" | 1.5 | 0.7968 | 19.31 | 0.7897 | 19.29 |
| 80/60/BG | After_ 10" | 1.5 | 0.9888 | 34.98 | 0.8426 | 24.35 |
| 80/60/BG | Before | 3.0 | 0.6776 | | 0.6720 | |
| 80/60/BG | After_ 2" | 3.0 | 0.7987 | 15.16 | 0.7962 | 15.60 |
| 80/60/BG | After_ 5" | 3.0 | 0.8497 | 20.25 | 0.8475 | 20.71 |
| 80/60/BG | After_ 7" | 3.0 | 0.8200 | 17.37 | 0.8169 | 17.74 |
| 80/60/BG | After_ 10" | 3.0 | 0.8601 | 21.22 | 0.8530 | 21.22 |
| 80/60/BG | Before | 5.0 | 0.6469 | | 0.6434 | |
| 80/60/BG | After_ 2" | 5.0 | 0.7897 | 18.08 | 0.7870 | 18.25 |
| 80/60/BG | After_ 5" | 5.0 | 0.8448 | 23.43 | 0.8421 | 23.60 |
| 80/60/BG | After_ 7" | 5.0 | 0.8373 | 22.74 | 0.8327 | 22.73 |
| 80/60/BG | After_ 10" | 5.0 | 0.8026 | 19.40 | 0.7975 | 19.32 |

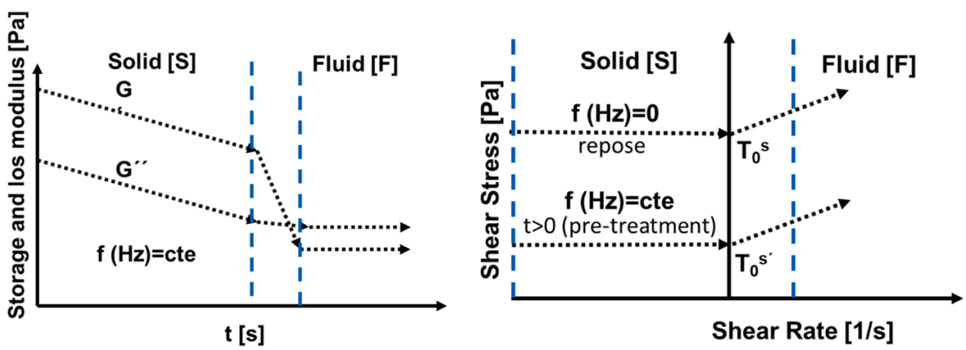


**Fig. 9.** Left. Schematic representation of the variation of the storage and loss modulus of the matrix submitted to a vibration during time. Right. Schematic representation of the reduction of $T_0^s$ of the matrix to $T_0^{s'}$after the pretreatment through oscillating magnetic field.

**Table 9**
Alignment index and mechanical efficiency factor of fiber aligned through a previous activation of same directional oscillatory magnetic field and simultaneous DMP in the same direction.

| **Pre-Alternating magnetic field + DMP** | | | | | | |
|---|---|---|---|---|---|---|
| Fibre | Sequence+ Exp Time (s) | Intensity (A) | Alignment Index | Improvement Alingm.index (%) | Efficiency rate | Improvement Eff.Rate (%) |
| 80/60/BG | Before | 1.5 | 0.6288 | | 0.6247 | |
| 80/60/BG | After_ 2" | 1.5 | 0.7359 | 14.55 | 0.7294 | 14.35 |
| 80/60/BG | After_ 5" | 1.5 | 0.7916 | 20.57 | 0.7856 | 20.48 |
| 80/60/BG | After_ 7" | 1.5 | 0.7868 | 20.08 | 0.7806 | 19.97 |
| 80/60/BG | After_ 10" | 1.5 | 0.8036 | 21.75 | 0.7960 | 21.52 |
| 80/60/BG | Before | 3.0 | 0.6391 | | 0.6355 | |
| 80/60/BG | After_ 2" | 3.0 | 0.8510 | 24.90 | 0.8468 | 24.95 |
| 80/60/BG | After_ 5" | 3.0 | 0.8454 | 24.40 | 0.8393 | 24.28 |
| 80/60/BG | After_ 7" | 3.0 | 0.7970 | 19.81 | 0.7956 | 20.12 |
| 80/60/BG | After_ 10" | 3.0 | 0.8249 | 22.52 | 0.8182 | 22.33 |
| 80/60/BG | Before | 5 | 0.6047 | | 0.5987 | |
| 80/60/BG | After_ 2" | 5.0 | 0.8102 | 25.36 | 0.8041 | 25.54 |
| 80/60/BG | After_ 5" | 5.0 | 0.8253 | 26.73 | 0.8198 | 26.97 |
| 80/60/BG | After_ 7" | 5.0 | 0.8493 | 28.80 | 0.8478 | 29.38 |
| 80/60/BG | After_ 10" | 5.0 | 0.8262 | 26.81 | 0.8207 | 27.05 |

direction of the reinforcement with the main stresses, which causes cracking perpendicular to it. It also will lead to composites with higher mechanical resistance and more ductile, what can also reduce the need for reinforcement VF or the increase of ultimate loads and dynamic situations.

The study here presented has been done with an OMF which generated a magnetic torque under the rheological torque, what only may cause stress in the solid region of the matrix. More advances in the research can be done, if the OMF overpasses the $T_0^s$. The results in fiber aligning mechanical efficiency with a higher OMF may be higher as the matrix passes from solid to liquid, what is supposed to present nule $T_0$ in the moment of DMP shot [37].

Further research can be made to consider if the use of two perpendicular coils is better that the use of only one coil, but the time after OMF pretreatment should be reduced by the design of a shotting system coordinating both outputs. Moreover, the system can be also implemented in samples with conventional reinforcement to analyze the mechanical combination of both systems in real scale beams. OMF+DMP can be also studied in composites with polymeric matrices such as resins, reinforced with metallic fibers or polymeric fibers with ferromagnetic coating.

## 5. Conclusions

The use of a combined system of magnetic fields to align fibers in composites with rheological behavior similar to cementitious materials has been presented. This system not only consider the magnetic forces to rotate the fiber in a matrix but also modifies the rheological properties of the matrix in which the fiber is immersed. For this, the matrix Yield Stress can be reduced using an Oscillatory Magnetic Field, which in a process of load and unload, affects the bonds in the microstructure. This process has been to be also effective even in the elastic range of a viscoelastic material such as Carbopol. This behavior can be modified at different frequencies and with the use of different additions to modify the rheology behavior of the cementitious matrix.

OMF can be combined with DMP also simultaneously, what in fact is desirable as the matrix has no time to recover its rheological properties. This means that the coordination of OMF and DMP is needed to have better results. Coils can be limited in size and magnetic fields and with this combination of OMF and DMP the device can be use in matrices with high yield stress or viscosity.

The use of OMF and DMP with two pairs of perpendicular coils can facilitate the manufacturing process and the electrical and electronic design of the system as they are compatible and very effective.

The analysis of the time of exposure to OMF is suitable of specific study for each matrix, as so the DMP intensity. The results obtained with this system are encouraging to increase the possibilities of the use of magnetic fields to align fibers in matrices with different rheological behavior. The application of the system in precast can be suitable to samples incorporating the fibers combined with traditional reinforcement, especially in beams and special samples for joints designed to work under dynamic loads to optimize the design not only from the shape or inertia but also from the internal distribution of the reinforcement.

### CRediT authorship contribution statement

**Nelson Flores Medina:** Writing – review & editing, Writing – original draft, Supervision, Resources, Project administration, Investigation, Formal analysis, Data curation, Conceptualization. **Laura Trigo Ramirez:** Writing – review & editing, Writing – original draft, Methodology, Investigation, Formal analysis, Data curation, Conceptualization. **Víctor Pérez Villar:** Writing – review & editing, Writing – original draft, Methodology, Investigation, Formal analysis, Data curation, Conceptualization. **Víctor M. Cabrera García:** Visualization, Data curation. **Francisco Gil Carrillo:** Visualization.

### Declaration of Competing Interest

The authors declare the following financial interests/personal relationships which may be considered as potential competing interests: Nelson flores medina reports financial support and administrative support were provided by Ministry of Science Technology and Innovations. If there are other authors, they declare that they have no known competing financial interests or personal relationships that could have appeared to influence the work reported in this paper.

### Acknowledgement

This research was funded by the Spanish Science Ministery, Grant number PID2020–119707RB-I00 (ORIENTACIÓN DE FIBRAS DE REFUERZO EN HORMIGÓN PARA EDIFICACIÓN MEDIANTE CAMPOSMAGNÉTICOS). The support from the Universidad de las Palmas de Canaria, and especially the help of the building construction and structures laboratory of Escuela de Arquitectura de Las Palmas de Gran Canaria, in also highly acknowledged.

*Conflict of Interest*

The authors declare that they have no known competing financial interests or personal relationships that could have appeared to influence the work reported in this paper.

### Data Availability

No data was used for the research described in the article.

### References

[1] Naaman and H.W. Reinhardt, 1996, High performance fiber reinforced composites, ISBN 0 419 21180 2.
[2] Doo-Yeol Yoo, Nemkumar Banthia, Mechanical properties of ultra-high performance fiber-reinforced concrete: A review, Cem. Concr. Compos. 73 (2016) 267–280.
[3] Kalaimani Markandan, Chang Quan Lai, Fabrication, properties and applications of polymer composites additively manufactured with filler alignment control: A review, Compos. Part B 256 (2023) 110661.
[4] Huanghuang Huang, et al., Improvement effect of fiber alignment on resistance to elevated temperature of ultra-high performance concrete, Compos. Part B: Eng. 177 (2019) 107454.
[5] Laetitia Martinie, et al., Rheology of fiber reinforced cementitious materials: classification and prediction, Cem. Concr. Res. 40 (2010) 226–234, 2010.
[6] L. Nachbaur, et al., Dynamic mode rheology of cement and tricalcium silicate pastes from mixing to setting, Cem. Concr. Res. 31 (2001) 183–192.
[7] A.M. Mostafa, A. Yahia, New approach to assess build-up of cement-based suspensions, Cem. Concr. Res. 85 (2016) 174–182.
[8] Q. Yuan, et al., On the measurement of evolution of structural build-up of cement paste with time by static yield stress test vs. small amplitude oscillatory shear test, Cem. Concr. Res. 99 (2017) 183–189.
[9] Michael Haist, et al., Interlaboratory study on rheological properties of cement pastes and reference substances: comparability of measurements performed with different rheometers and measurement geometries, Mater. Struct. 53 (2020) 92.
[10] Shweta Sharma, et al., Viscoelasticity and rheological hysteresis, J. Rheol. 67 (2023) 139–155.
[11] Ye Qian, Shiho Kawashima, Flow onset of fresh mortars in rheometers: Contribution of paste deflocculation and sand particle migration, Cem. Concr. Res. 90 (2016) 97–103.
[12] Mohammad Hajforoush, et al., Investigation of engineering properties of steel fiber reinforced concrete exposed to homogeneous magnetic field, Constr. Build. Mater. 252 (2020) 119064.
[13] Iman Abavisani, et al., Oscillatory magnetic field effect on fine-aggregate steel chip–reinforced concrete properties, J. Mater. Civ. Eng. 30 (6) (2018).
[14] Fakhri Javahershenas, et al., Effect of magnetic field exposure time on mechanical and microstructure properties of steel fiber-reinforced concrete (SFRC), J. Build. Eng. 35 (2021) 101975.
[15] Igor da Silva Brito, et al., Flexural behavior of HPFRCC: Enhancing post-crack strength and toughness by magnetic alignment of the reinforcement, Constr. Build. Mater. 269 (2021) 121265.
[16] M.J.H. Wijffels, et al., Magnetic orientation of steel fibers in self-compacting concrete beams: effect on failure behaviour, Cem. Concr. Compos. 80 (2017) 342–355.
[17] Guodong Cao, et al., Experimental analysis and numerical simulation of flow behavior of fresh steel fiber reinforced concrete in magnetic field, Constr. Build. Mater. 347 (2022) 128505.
[18] Jacopo Ciambella, Magnetic alignment of short carbon fibres in curing composites, Compos. Part B 109 (2017) 129–137.
[19] Donglu Shi, et al., Magnetic alignment of Ni/Co-coated carbon nanotubes in polystyrene composites, Compos.: Part B 42 (2011) 1532–1538.
[20] Xiaowei Wang, et al., Flexural properties of a 2D-distributed steel fiber reinforced cement-based composite two-way slab, J. Build. Eng. 73 (2023) 106792.
[21] Kristýna Carrera, et al., The effect of magnetic field parameters on fibre orientation in high-performance fibre-reinforced concrete, Mech. Mater. 177 (2023) 104534.
[22] Yongming Xiong, et al., Study on the electromagnetic field aligning steel fibres in UHPC reinforced beams: Effect, mechanism and flexural behavior, Cem. Concr. Compos. 143 (2023) 105251.
[23] Longbang Qing, et al., Research progress on aligned fiber reinforced cement-based composites, Constr. Build. Mater. 363 (2023) 129578.
[24] V.íctor P.érez Villar, Nelson Flores Medina, Alignment of hooked-end fibres in matrices with similar rheological behaviour to cementitious composites through homogeneous magnetic fields, Constr. Build. Mater. 163 (2018) 256–266.
[25] P. Coussot, Rheometry of Pastes, suspensions and granular materials: Applications in Industry, J Wiley & Sons, 2005.
[26] Sergiy Shyshko, Viktor Mechtcherine, Developing a Discrete Element Model for simulating fresh concrete: Experimental investigation and modelling of interactions between discrete aggregate particles with fine mortar between them, Constr. Build. Mater. 47 (2013) 601–615.
[27] E.Di Giuseppe, et al., Characterization of Carbopol® hydrogel rheology for experimental tectonics and geodynamics, Tectonophysics 642 (2015) 29–45.

[28] M. Hernández, et al., Rheological characterization of easy-to-disperse (etd) carbopol hydrogels, J. Dispers. Sci. Technol. 19 (1998) 31–42.

[29] Fabien Mahaut, et al., Effect of coarse particle volume fraction on the yield stress and thixotropy of cementitious materials, Cem. Concr. Res. 38 (2008) 1276–1285.

[30] N.I. Fisher, Statistical Analysis of Circular Data, Cambridge University Press, 1993. ⟨doi.org/10.1017/CBO9780511564345⟩.

[31] K.V. Mardia, P.E. Jupp, Directional Statistics, Willey Series in Probability and Statistics, first ed, John Wiley & Sons, Ltd., London, 2000. ⟨10.1002/9780470316979⟩.

[32] H. Krenchel, Fibre spacing Specif. Fibre Surf., Fibre Reinf. Cem. Concr. 1975 (1975) 69–79.

[33] Bryan Harris, Engineering Composite Materials, Taylor and Francys, 1999. ISBN: 9781861250322, 1861250320.

[34] Théau Conte, Mohend Chaouche, Rheological behavior of cement pastes under large amplitude oscillatory shear, Cem. Concr. Res. 89 (2016) 332–344.

[35] Eliane Younes, et al., On the elusive nature of Carbopol gels: "model", weakly thixotropic, or time-dependent viscoplastic materials? J. Non-Newton. Fluid Mech. 281 (2020) 104315.

[36] Ye Qian, Shiho Kawashima, Use of creep recovery protocol to measure static yield stress and structural rebuilding of fresh cement pastes, Cem. Concr. Res. 90 (2016) 73–79.

[37] Noemi Baldino, et al., Rheological behaviour of fresh cement pastes: Influence of synthetic zeolites, limestone and silica fume, Cem. Concr. Res. 63 (2014) 38–45.

[38] V.íctor Pérez Villar, et al., 'Correlation through directional statistics of the consequences of magnetic alignment of steel fibers immersed in metaphor fluids of cementitious matrices', Constr. Build. Mater. (2024) 444.

[39] A. Raju, M. Shanmugaraja, Recent researches in fiber reinforced composite materials: A review, Mater. Today.: Proc. 46 (2021) 9291–9296. International Mechanical Engineering Congress 2019.

[40] Z. Jaworski, T. Spychaj, A. Story, G. Story, Carbomer microgels as model yield-stress fluids, Rev. Chem. Eng. 38 (7) (2022) 881–919.